Bioorg. Med. Chem. 44 (2021) 116296

Contents lists available at ScienceDirect

Bioorganic & Medicinal Chemistry

journal homepage: www.elsevier.com/locate/bmc

Dithiolated peptides incorporating bis(tryptophan)s for cooperative mercury(II) binding

Maria Ngu-Schwemlein [a,*], John Merle [a], T'ea Cameron [a], Charlexia Witcher [a], Daniel Todd [b]

[a] Department of Chemistry, Winston-Salem State University, Winston-Salem, NC 27110, USA
[b] Department of Chemistry and Biochemistry, University of North Carolina at Greensboro, Greensboro, NC 27402, USA

ARTICLE INFO

Keywords:
Mercury poisoning
Mercury-peptide complexes
Cation-π interaction
Computational modeling, density functional theory

ABSTRACT

The indole side chain of tryptophan is a versatile π-donor that can participate in various types of cation-π interactions. An understanding of how it may contribute as an auxiliary binding group in mercury(II) complexes can provide valuable insights toward the design of effective chelators for optimal mercury immobilization. In this study, we investigate how the incorporation of two tryptophan residues in model dicysteinyl peptides might participate in peptide-mercury(II) complex stabilization. Two pentapeptides consisting of a Cys-Trp-Cys sequence motif containing a second tryptophan residue at the *N*-terminal (**BT1**) or C-terminal (**BT2**) were designed. An analogous cyclohexapeptide (**BT3**) was included to evaluate how tryptophan residues, restricted in constrained peptidic turn motifs, might take part in mercury(II) complexation. Their interactions with mercury(II) were investigated by spectroscopic methods and computational modeling. UV–vis studies indicate the formation of 1:1 dithiolated mercury(II) complex, which is corroborated by ESI-MS analysis. Spectroscopic studies reveal that the tryptophan indole group(s) in **BT1** and **BT3** can participate in mercury(II) cation-π interactions. Optimized 1:1 mercury(II)-**BT3** structures indicate that both indole rings are very close to the mercury(II) coordination site and could stabilize it by shielding it from ligand exchange. These findings provide some useful insights toward use of aromatic donor groups as hydrophobic shields in designing more effective metal chelating agents.

1. Introduction

Mercury is a well-known environmental toxin and it is considered by the World Health Organization (WHO) as one of the top ten chemicals of major public health concern.[1] Exposure to the various forms of mercury can detrimentally affect the brain, kidney, and lungs, resulting in neurotoxicity, hepatotoxicity, nephrotoxicity, and pulmonary toxicity.[2] The effects of organic mercury in the nervous system is linked to its oxidized form, mercury(II), which binds to critical intracellular sites and thereby alters and inhibits some protein functions, resulting in persistent neurological impairements.[3–4] Today, the common clinical drugs for chelation therapy arising from mercury poisoning are dimercaptosuccinic acid (DMSA) and dimercaptopropane-sulfonic acid (DMPA). However, it has been reported that these are not well-optimized molecules for mercury chelation.[5] Furthermore, their mercury complexes are not necessarily stable *in vivo* and they can undergo ligand exchange reactions with other free thiols of similar reactivities.[6–7] Consequently, the binding of mercury(II) to biological ligands such as cysteine can mediate multiple toxic effects such as inhibitory effects on enzymes resulting in apoptosis, oxidative stress, or inflammation.[4] Therefore, it is worthwhile to pursue mercury(II) chelators that will form stable complexes to prevent mercury(II)-thiol exchange reactions with endogenous biological ligands.

Metal binding proteins usually share a common characteristic feature: the metal is ligated by hydrophilic donor atoms/groups that are embedded within a shell of hydrophobic groups.[8] It has been suggested that the latter could increase their stability by creating an axial hydrophobic fence, which could shield it from exchanges with nearby water molecules.[9] Some of these metalloproteins contain aromatic rings of tryptophan, tyrosine, or phenylalanine that are situated very close to the metal coordination center.[10] These non-covalent aromatic interactions can play an important role in the stability and function of these metalloproteins. Dougherty et al. have reported various experimental and theoretical studies on related aromatic π and cation interactions and provided an understanding of the nature of these non-covalent bond types.[11–13] Cation-π interactions between the tryptophan indole ring and cationic groups are increasingly recognized as an important electrostatic interaction and are employed in the rational design of chemosensors for

* Corresponding author at: 601 M.L. King Jr. Drive, W.B. Atkinson Science Bldg, Winston-Salem, NC 27110, USA.
E-mail address: Schwemleinmn@wssu.edu (M. Ngu-Schwemlein).

https://doi.org/10.1016/j.bmc.2021.116296
Received 12 April 2021; Received in revised form 10 June 2021; Accepted 20 June 2021
Available online 27 June 2021

metal ions and some therapeutics.[14–20] Accordingly, we have incorporated it in the design of stable mercury(II)-peptide complexes. Previous studies from our group showed that a single indole ring in a pentapeptide, GCWCG, can participate in cation-π interaction to stabilize the mercury(II)-pentapeptide complex.[21] In continuation of this work, the present study was undertaken to investigate how two tryptophan residues might participate in complex formation with mercury(II). Pentapeptides containing bis(tryptophan) residues, WCWCG (**BT1**) and GCWCW (**BT2**) were selected to evaluate the optimal position of the second tryptophan residue to maintain mercury(II) cation-π interaction. We anticipated that an effective hydrophobic shield could constitute a dithiolated mercury coordination site that would be 'sandwiched' between two indole rings. Cyclohexapeptide CWCGWG (**BT3**) was selected for this study because head-to-tail cyclopeptides with reverse turn motifs could provide a structurally more defined molecular scaffold that could organize the two tryptophan indole rings for effective shielding on opposite sides of the coordination site. Its symmetric primary sequence was selected by adding a glycine residue to **BT2** to amplify conformational preferences toward secondary structural preorganization.

Herein, we describe the characterization of 1:1 dithiolated mercury peptide complexes with S-Hg coordinate bond formation by UV–vis spectroscopy and electrospray ionization mass spectrometry (ESI-MS). Spectroscopic signatures for cation-π interactions were evaluated by UV–vis and circular dichroism (CD) spectroscopy. The fluorescence emission properties of the indole rings in these peptides were also studied to investigate how they might interact with the coordinated mercury. Furthermore, the structure of the 1:1 mercury(II) and **BT3** complex was explored by computational calculations to understand how the two indole groups in the cyclohexapeptide scaffold could be involved in complex formation. The findings of this work will be useful for the rational design of more effective compounds to immobilize heavy metal ions, and provide useful insights to explore opportunities for peptides in drug discovery.

2. Results and discussion

2.1. Electrospray-ionization mass spectrometry (ESI-MS) of the mercury and peptide complexes

The nature and stoichiometry of the mercury complexes formed with each peptide (**BT1, BT2, and BT3**) was first investigated qualitatively by electrospray-ionization mass spectrometry (ESI-MS). Figure 1 shows the ESI-MS spectra corresponding to reaction mixtures containing a 1:1 ratio of mercury(II) to peptide in ammonium formate buffer at pH 7. They show that the 1:1 complex is the only predominant complex formed for these three peptides. Insets in Fig. 1 show the mercury isotopic pattern for these 1:1 mercury-peptide complexes. These monocharged molecular ion adducts show *m/z* values corresponding to double deprotonations, which can be attributed to deprotonations from two cysteinyl thiols because mercury(II) is known to have a high affinity for the sulfur atoms in thiol compounds.[22] Cationized sodium and potassium adducts of these molecular ions and the parent ions are also detected. These non-specific binding of common solution phase cations to peptides are the products of gas phase ion–molecule interactions.[23–24] The uncharged cyclopeptide **BT3** also shows an adduct corresponding to cationization with an ammonium ion that is derived from the ammonium formate buffer. We also compared the mercury(II) complex formation tendencies with analogous pentapeptides containing one or no tryptophan residue, GCWCG and GCGCG, respectively.[21] In contrast, these peptides showed multiple molecular ion adducts corresponding to 1:1, 1:2, and 2:2 mercury-peptide complexes, as well as free peptide dimers (Fig. S1).

From the above comparative analysis, it is evident that the peptides

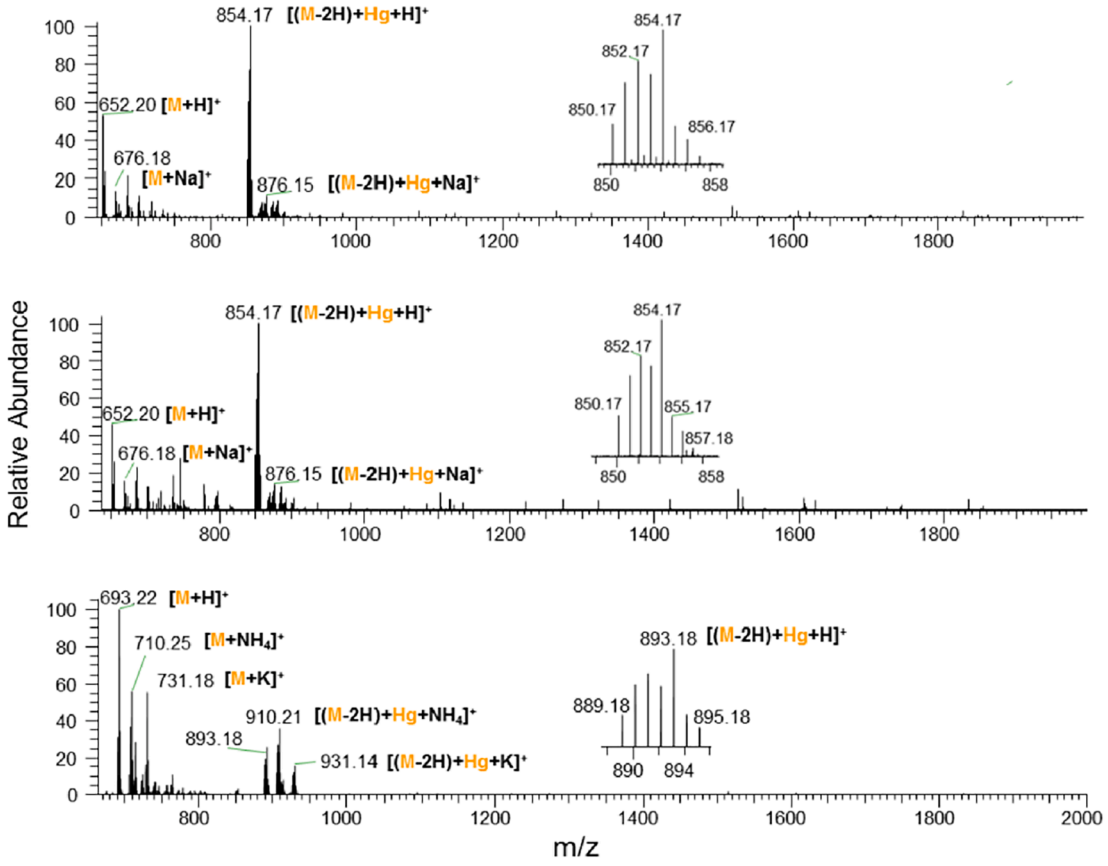

Figure 1. Electrospray ionization mass spectra of reaction mixtures containing 1 to 1 ratio of Hg(II):peptides for (a) **BT1**, (b) **BT2**, and (c) **BT3**. Insets show mercury isotopic patterns for detected mercuriated peptide adducts.

containing two tryptophan residues (**BT1-3**) tend to form only 1:1 complexes with mercury(II), whereas analogous peptides with one or no tryptophan residues also form other complexes. It is conceivable that two tryptophan indole rings can better stabilize the 1:1 mercury-peptide complex via intramolecular interactions, and avert formation of complexes with higher stoichiometric ratios.

2.2. UV–vis absorption spectrometry

The UV absorption spectra of mercury-thiolate complexes are characteristic of the type of mercury coordination. The ligand-to-metal charge transfer (LMCT) band for S—Hg bonds in linear dithiolated mercury absorb at relatively higher energy transitions (<240 nm) whereas the trigonal coordinated complexes exhibit absorbance at distinctly lower energy transitions (240–300 nm).[25–26] The UV absorption spectrum of tryptophan is dominated by the indole chromophore, which gives rise to the L_b (~280 nm), L_a (~270 nm), B_b (~220 nm) and B_a (~200 nm) bands. The strong B_b absorption is sensitive to its environment, and a small red shift accompanied by decreasing intensity have been associated with cation-π interaction.[18–19, 27] Figure 2a shows the UV spectra of **BT1** following titrations with mercury(II). The B_b absorption of its indoles at ~220 nm is overlapping with another band around 205 nm (n-π* transitions of the peptide bonds). The observed increase in intensity at 205 nm reflects changes in the peptide backbone when **BT1** interacts with mercury(II). As a result, the effect of mercury (II) binding on the weakening in intensity of the B_b band is obscured due to its overlap with the 205 nm band. Figure 2b shows the corresponding UV difference absorption spectra. Additions of mercury(II) resulted in the formation of a new band at ~234 nm that linearly increased with titrations with mercury(II) up to 1 equiv (inset). This band is characteristic of LMCT transition for dithiolated mercury(II), and is similar to that reported for an analogous pentapeptide containing one tryptophan residue (GCWCG).[21] However, it is red shifted by ca. 7 nm compared to the pentapeptide containing only one tryptophan. It is conceivable that this LMCT band shift could be due to changes in the B_b absorption of both indole rings when **BT1** binds mercury.

BT1 also shows changes in its indole L_a (~270 nm) and L_b (~280 nm) absorption bands, which resulted in a negative absorption difference band in the 280 nm region. These low-energy transitions of indole are sensitive to changes in polarity and therefore, these spectral changes are indicative of changes in the local environment of the indole ring following complex formation. In contrast, changes in these indole L_a and L_b absorption bands were not observed in our previous study on pentapeptides containing only one tryptophan residue.[21]

Figure 3 shows the UV absorption difference spectra for **BT2**. Titrations with mercury(II) yielded similar results as observed for **BT1**. Figure 4 shows the UV spectral data for the cyclohexapeptide **BT3**. Notable spectral differences from **BT1** and **BT2** include a three-fold increase in intensity of the absorption difference band at 232 nm and the formation of a positive difference band at 295 nm. In contrast to **BT1** and **BT2**, which exhibited a linear intensity increase at 234 nm, the analogous band for **BT3** at 232 nm followed a polynomial regression fit for two variables (Fig. 4 inset). Additionally, its absorption difference band at 295 nm is positive whereas **BT1** and **BT 2** exhibited negative bands. These observed spectral differences for **BT3** indicate that its indole rings are undergoing significant changes in its local environment following complex formation but somewhat different from that experienced by **BT1**, **BT2**, and the previously reported pentapeptides.[21]

In the presence of mercury(II) in excess of 1:1 mol equiv, all of these bis(tryptophan) peptides show a dramatic increase in UV absorbance, which could be due to the formation of polynuclear species consisting of complexes with higher stoichiometric ratios. **BT2** and **BT3** also tend to form species that are not very soluble, resulting in turbid solutions that increase UV absorption drastically.

The above UV spectral data indicate that **BT1-3** form 1:1 dithiolated mercury peptide complexes in reaction mixtures at pH 7. Although the

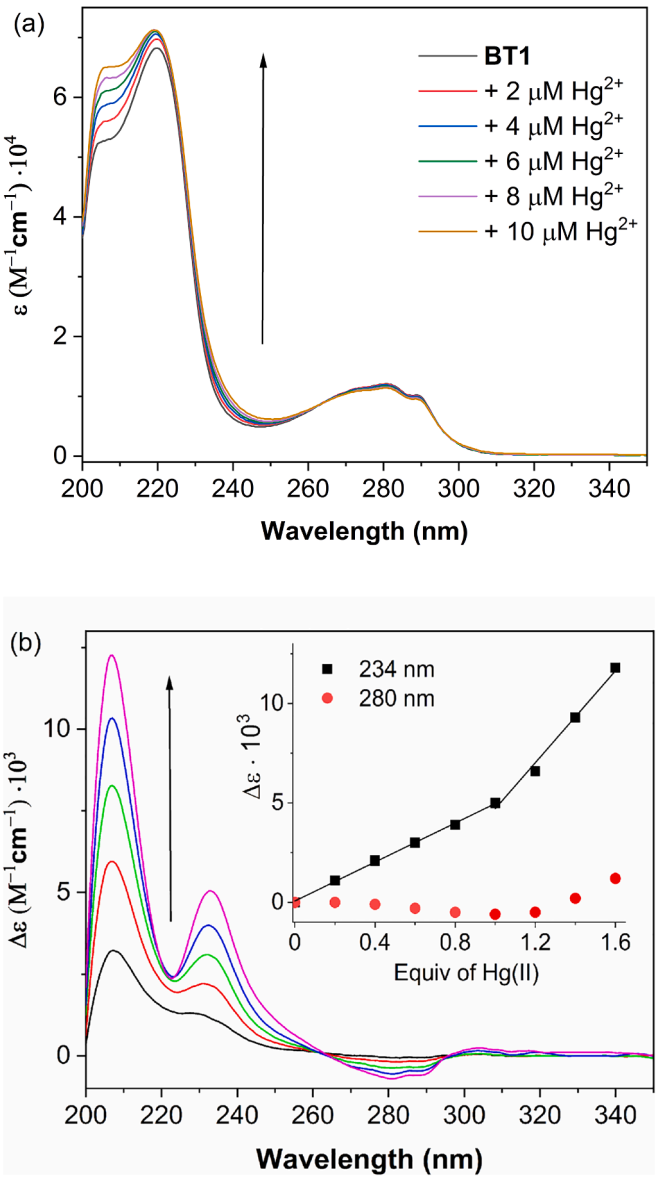

Figure 2. (a) UV spectra of **BT1** following titrations with increasing mole equiv of $HgCl_2$. (b) UV absorption difference spectra [$\Delta\varepsilon = \varepsilon(Hg\mathbf{BT1}) - \varepsilon(\mathbf{BT1})$] for **BT1**. Inset shows changes in extinction coefficient values versus mole equiv of $HgCl_2$ added, indicating 1:1 stoichiometry of the complex.

acidity of the cysteinyl thiol group (pK_a ca. 8) is expected to affect their binding to mercury(II), Pires et al. have previously shown that 1:1 dithioloated mercury peptides [Hg(CdPPC) and Hg(CPPC)] are formed at low pH values, and are stable up to pH 10.[28] In a separate study on an analogues pentapeptide (GCGCG), we also observed no significant changes in the extinction coefficient at 220 nm over the pH range 2 to 8 (unpublished work).

2.3. Circular dichroism

Circular Dichroism (CD) provides a good spectroscopic probe for peptide ligand interactions. The tryptophan aromatic indole side chain contributes to mid-UV CD, and changes in the 225–300 nm region provide a useful indication of ligand binding.[29] For example, Yorita et al. reported the development of a negative CD band at 223 nm which is characteristic of copper(II) and tryptophan indole cation-π interaction.[27]

Figure 5a shows the CD spectral changes of **BT1** following titrations with mercury(II). Inset shows the linear evolution of the CD signals at

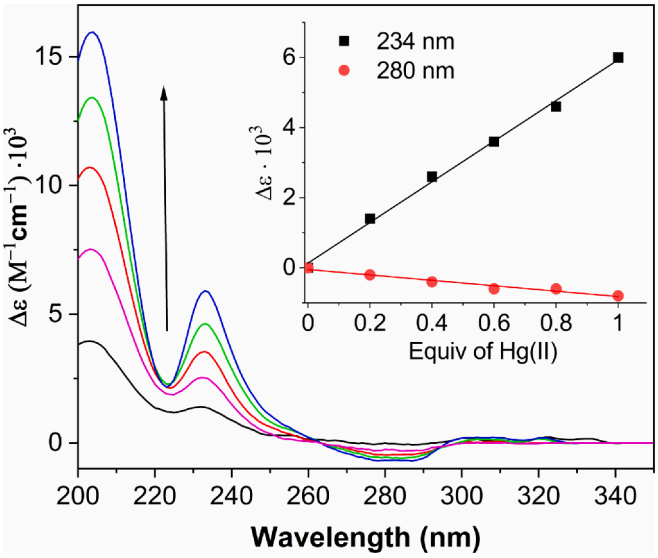

Figure 3. UV absorption difference spectra [Δε = ε(Hg**BT2**) - ε(**BT2**)] correspond to **BT2** titrated with increasing mole equiv of $HgCl_2$. Inset shows changes in extinction coefficient values at 234 nm and 280 nm versus mole equiv of $HgCl_2$ added.

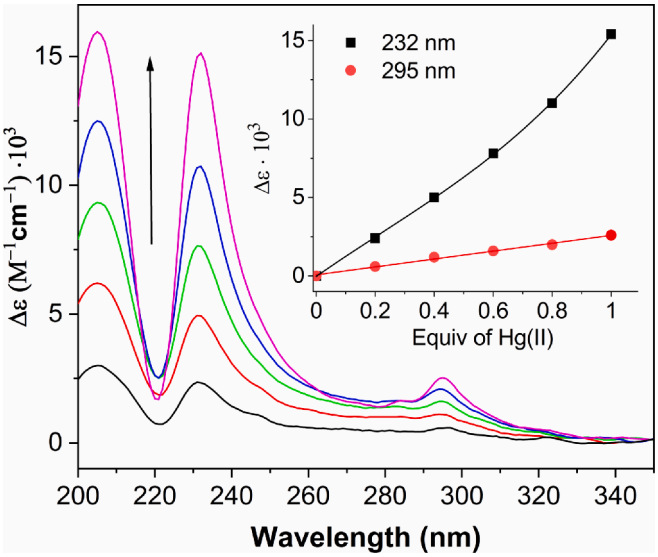

Figure 4. UV absorption difference spectra [Δε = ε(Hg**BT3**) - ε(**BT3**)] corresponding to **BT3** titrated with increasing mole equiv of $HgCl_2$. Inset shows changes in extinction coefficient values at 232 nm and a polynomial regression fit ($y = b_1x + b_2x^2$). Changes at 295 nm versus mole equiv of $HgCl_2$ added followed a linear regression fit.

208 nm and 232 nm up to 1.0 mol equiv of mercury(II). Changes in the 190–225 nm region reflect secondary structural changes in the peptide following mercury(II) binding to the cysteinyl thiolates. The build-up of a positive CD band centered at 208 nm indicates changes in the peptide backbone that is characteristic of β-turn formation.[30] In addition, the small positive band at 228 nm, which is contributed by the aromatic indoles, undergoes a small blue shift. This is accompanied by the development of a negative CD band at 232 nm. Together, these changes are indicative of perturbations of one or both tryptophan indole rings in **BT1** following mercury(II) binding. Notably, the formation of the negative band at 232 nm is characteristic of metal cation-π interaction as previously reported.[27] However, it is red-shifted by ca. 10 nm when compared to the corresponding negative CD band exhibited by the

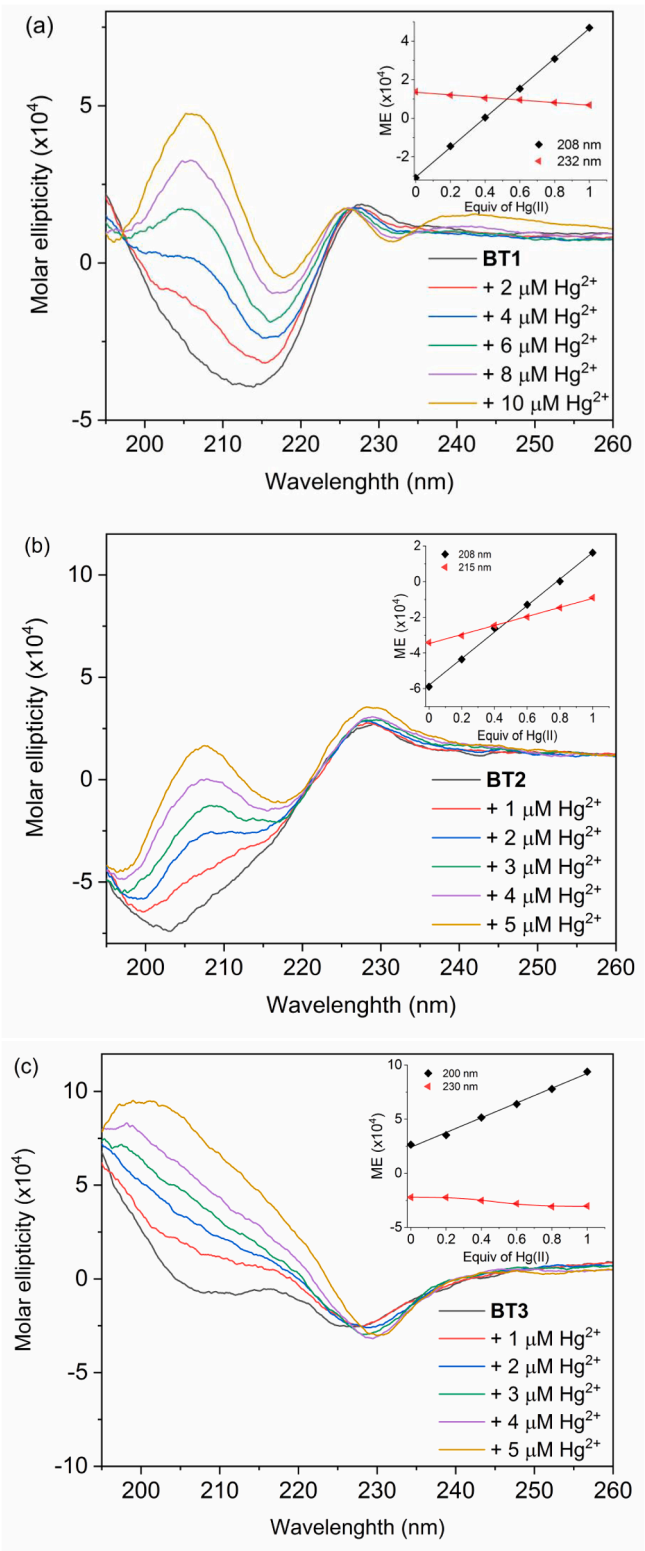

Figure 5. Circular dichroism spectra of (a) **BT1**, (b) **BT2**, and (c) **BT3** following titrations with increasing mole equiv of $HgCl_2$. Inset shows the change in molar ellipticity value at indicated wavelengths versus mole equiv of $HgCl_2$ added.

pentapeptide containing one tryptophan residue.[21] This band shift is consistent with the aforementioned UV red-shift in the B_b transition of **BT1** following mercury complex formation. The above CD data and the observed UV spectral changes in the B_b, L_a, and L_b absorption bands in **BT1** (Fig. 2b) are consistent with cooperative mercury(II) binding by the

tryptophan indole rings. These CD spectra also exhibit isodichroic points at 195 nm and 227 nm, which suggest a two-state structural transition between the unbound and mercury(II) bound **BT1**. The absence of a positive n-σ* S—S transition band between 260 nm and 320 nm indicates that the cysteinyl thiols were not oxidized to form disulfide bonds.

BT2 exhibits similar secondary structural changes as shown by **BT1** following titrations with mercury(II). This is depicted by the formation of a positive band at 208 nm and a negative band at 215 nm as shown in Fig. 5b. In contrast, the small positive band at 228 nm did not undergo a blue shift and no negative CD band formed at ca. 230 nm. Instead its intensity increased following titration with 1:1 mol equiv of mercury(II). These spectral changes indicate that the indole groups in **BT2** are experiencing some changes in their environment that are different from that in **BT1**.

Figure 5c shows the CD spectral changes of **BT3** following titrations with mercury(II). Although **BT3** has a head-to-tail cyclic peptide backbone that restricts its structural flexibility, significant CD spectral changes in the 190 and 220 nm region, following titrations with mercury (II), show that **BT3** did not adopt a pre-organized secondary structure before binding mercury(II). Notably, the negative tryptophan B_b band at 227 nm also undergoes a red-shift and an increase in intensity as observed for **BT1**. These changes in the tryptophan B_b CD band and its corresponding B_b, L_a, and L_b UV absorption bands indicate that the indole rings in **BT3** could be undergoing mercury cation-π interactions.

2.4. Steady state fluorescence spectroscopy

Heavy metal cation-π interactions are known to quench the fluorescence of some aromatic hydrocarbons due to the formation of a non-fluorescent complex.[31] For example, Xue et al. reported that when an indole ring establishes cation-π interaction with Cu(II) in the copper chaperone protein CusF, it quenches its fluorescence emission.[32] Therefore, fluorescence quenching measurements can be used to assess the accessibility of mercury(II) to the tryptophan indoles via cation-π interactions in **BT1**, **BT2**, and **BT3**. Additionally, any significant contribution from quenching that arises from diffusive encounters between mercury(II) and the tryptophan indoles can be assessed by temperature studies.[33]

Figure 6 shows the fluorescence emission spectra of these peptides following titrations with mercury(II). About 70% of their intrinsic fluorescence was quenched after adding 1 equiv of mercury(II). Insets in these figures show the Stern-Volmer plots for the quenching of tryptophan fluorescence emission at 25°C, 35°C, and 45°C. These plots show a consistent upward curvature, indicating that one or both tryptophan indoles are experiencing a mixture of static quenching, due to complex formation, and dynamic quenching as a result of diffusive encounter with mercury(II). However, **BT1** and **BT3** did not show any temperature dependency in these plots, indicating that the contribution from static quenching is more significant than dynamic or collisional quenching. On the other hand, the Stern-Volmer plots for **BT2** showed an increase in fluorescence quenching at higher temperatures and hence larger amounts of collisional quenching.

The above fluorescence results indicate that the tryptophan indole rings of **BT1** and **BT3** can participate more effectively in cation-π interactions with the coordinated mercury(II) than **BT2**. This is consistent with the corresponding CD spectral studies as described in section 3.2, whereby **BT2** did not exhibit any signature mercury cation-π CD band. In pentapeptide **BT2**, the second tryptophan residue is positioned at the C-terminal whereas in **BT1**, it is at the *N*-terminal end of the pentapeptide. The C-terminal tryptophan indole group could more readily undergo intramolecular cation-π interaction with its *N*-terminal ammonium group because mercury binding by the cysteinyl thiolates would have resulted in a reverse peptide backbone turn. Consequently, the C-terminal tryptophan residue would be in close proximity to its *N*-terminal group for intramolecular ammonium cation and indole π interaction. On

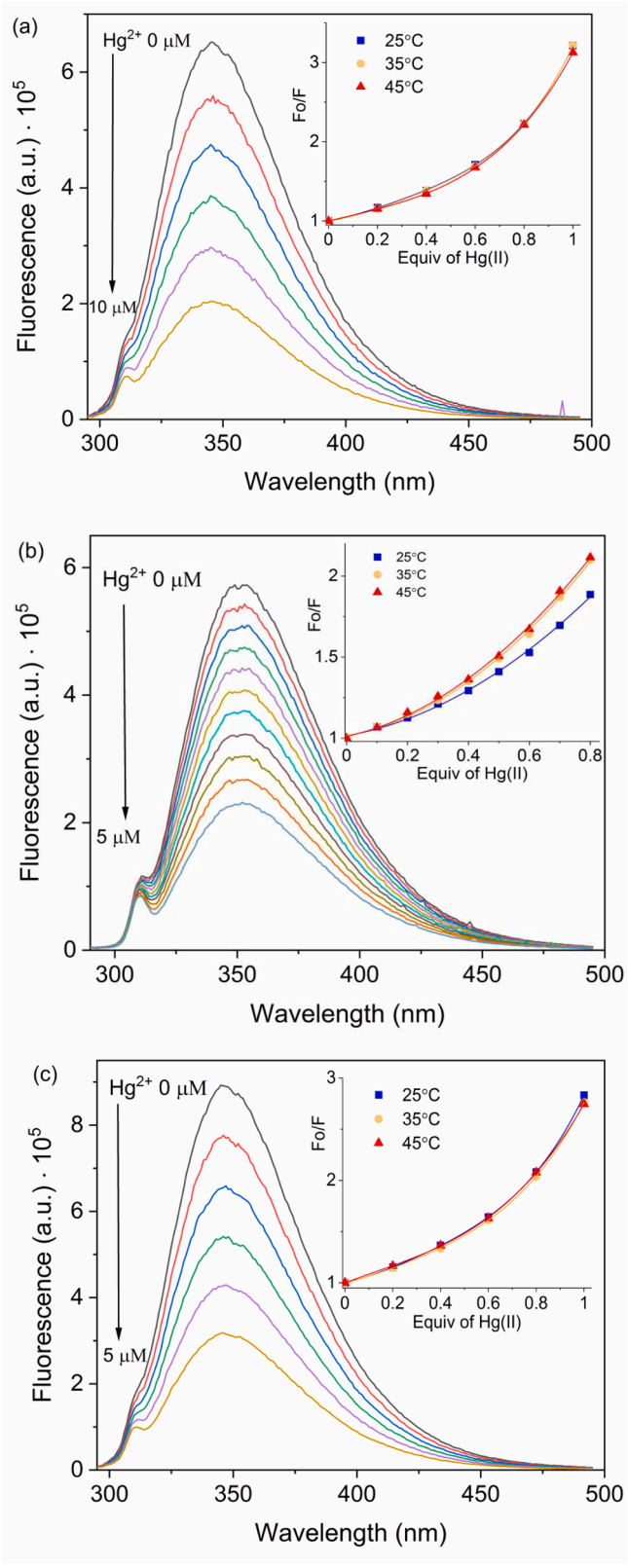

Figure 6. Fluorescence emission spectra of (a) **BT1**, (b) **BT2**, and (c) **BT3** following titrations with mercury(II) at 20°C. Inset: Stern-Volmer plots at 25°C, 35°C, and 45°C.

the other hand, the *N*-terminal tryptophan indole group of **BT1** cannot interact with its ammonium group due to torsional constraints and thus, its indole group could more readily participate in mercury cation-π interaction.

BT1 and **BT3** exhibit similar fluorescence quenching spectral data as that shown by the previously reported pentapeptide (GCWCG),[21] which could participate in mercury cation-π interaction to stabilize its complexation with mercury(II). This indicates that similarly, the tryptophan indole rings in **BT1** and **BT3** could interact with their respective coordinated mercury(II).

2.5. Computational modeling

The reduction in the number of possible conformational states in cyclopeptides compared to its linear analogs make them suitable for conformational analysis. Therefore, the effect on complex stability provided by tryptophan indole rings in 1:1 Hg-**BT3** complexes was studied by analyzing conformations of the Hg-**BT3** complex using density functional theory (DFT) methods. Conformations found with Gibbs energy in solution (G_{soln}) within 5 kJ/mol of the lowest are provided in Fig. 7. The B3LYP-D3 gas-phase molecular energy ($E_{B3LYP\text{-}D3}$), zero-point vibrational energy (E_{ZPV}), thermal correction to the Gibbs energy (G_{corr}), Gibbs energy of solvation (ΔG_{solv}), Gibbs energy in solution (G_{soln}) and relative Gibbs energy in solution for each complex in Fig.7 are provided in Table 1. Coordinates and select Gaussian file output data for all structures in Fig. 7 are provided in the supplementary information Table S1.

Each conformation (Fig. 7) includes two S—Hg bonds with lengths of ~ 2.40 Å and an S—Hg—S angle typically of 172°. These structural values are in agreement with values we and others have observed for similar mercury(II) sulfur complexation.[34] The most stable structures adopt a peptide ring conformation with two β -turns and two amide (N—H) to amide (C═O) hydrogen bonding interactions across the macrocyclic ring. The β-turn in the GCWC segment is most consistent with a Type IV turn ($\phi_{i+1} = 79.5°$,$\psi_{i+1} = 0.8°$,$\phi_{i+2} = 111.6°$,$\psi_{i+2} = 14.6°$; O—H—N = 2.09 Å for Conformer 1) and the β-turn GWGC segment is most consistent with a Type I' turn ($\phi_{i+1} = 58.1°$, $\psi_{i+1} = 31.7°$, $\phi_{i+2} = 116.1°$, $\psi_{i+2} = -22.3°$; O—H—N = 2.01 Å for Conformer 1).[35] In all the structures (Fig. 7), the amide groups of the tryptophan residues are in the β-turn and oriented the same. The tryptophan amide between the cysteine residues has the N—H directed toward the mercury whereas the tryptophan amide between the glycine residues has the carbonyl directed toward the mercury. In each conformer, the pyrrolo N_{in}-H of the indole ring for the tryptophan between glycine residues is slightly bend out of the ring plane toward a sulfur at the complexation site giving a S—H-N_{in} distance of ~ 3— Å. This interaction results in the S—Hg bond length increasing for the involved sulfur (~2.41 Å vs. ~ 2.39 Å). The shortest distance between the mercury and this indole ring is ~ 3.3 Å to carbon 7 of its benzo subunit.

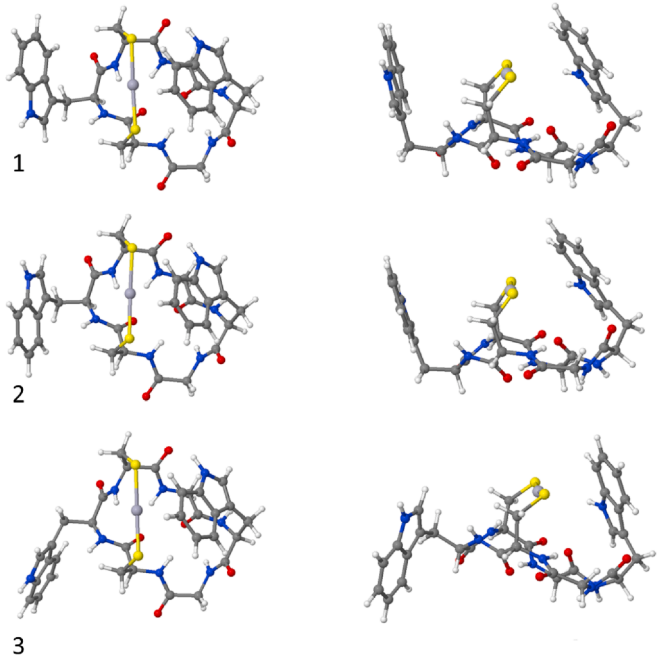

Figure 7. Most stable conformations found for the Hg-**BT3** complex. Left side = top view and right side = side view.

The difference between Conformers 1–3 is the orientation of the indole group for the tryptophan between the cysteinyl residues. The two most stable conformers have the indole oriented toward the complexation site. Of these two rotamers, Conformer 1 is 3.9 kJ/mol more stable than Conformer 2. This stabilization of Conformer 1 may be due to a favorable orientation of the indole dipole moment in relation to the nearby amide dipoles. The result being a smaller dipole moment of Conformer 1 (2.65 D) compared to Conformer 2 (3.93 D) to give a more negative Gibbs energy of solvation. Conformers 1 and 2 may gain stabilization, reflected in the lower $E_{B3LYP\text{-}D3}$ values (Table 1), relative to Conformer 3 from C—H—π interactions between the indole ring and Cys-C_β—H bonds. The electron rich aromatic indole ring can effectively interact with the electron poor Cys-C_β—H bond through C—H—π interactions. Such interactions have been observed in proteins and other alkyl-aromatic combinations.[36,37] Brandl et al. examined more than a 1000 structures in the Protein Data Bank and observed that most C—H—π interactions occur at distances between 3.5 and 4 Å.[38] Conformers 1 and 2 each have two Cys-C_β-H—indole distances in this range: Conformer 1 (3.25 Å and 3.57 Å) and Conformer 2 (3.09 Å and 4.05 Å). Conformer 3 has one Cys-C_β-H—indole distances in this range at 3.40 Å.

Structural details from the above energy-minimized structures indicate that the indole ring of the tryptophan between the glycine residues is oriented close to the coordination site to enable a mercury cation-π interaction as indicated by spectroscopic data described in sections 2.1–2.3. The indole group of the second tryptophan between cysteinyl residues is also oriented toward the complexation site as shown in the two most stable conformers (Fig. 7). These optimized structures show that the macrocyclic hexapeptide, consisting of two reverse-turn motifs, is a suitable molecular scaffold to organize two tryptophan indole rings for effective hydrophobic shielding on opposite sides of the dithiolated mercury ion.

3. Conclusion

The purpose of this work was to characterize the interactions of **BT1-3** with mercury(II) in order to investigate the possible involvement of two tryptophan indole rings in auxiliary binding to enhance peptide-mercury(II) complex stabilization. The UV spectroscopic data revealed that the dithiol groups in **BT1-3** form dithiolated S-Hg-S, which corresponds to the formation of 1:1 peptide-to-mercury complexes following titrations with mercury(II). This is corroborated by ESI-mass spectroscopic data. Circular dichroism data showed that the aromatic tryptophan indole ring(s) in **BT1** and **BT3** could participate in cation-π interaction with the thiolated mercury at the coordination site, and thereby could act as a hydrophobic shield to enhance chelation and immobilization of mercury. However, **BT2** did not show any signature CD band for metal cation-π interaction. It is likely that the C-terminal tryptophan indole readily interacted with its *N*-terminal ammonium group via ammonium cation-π. In conclusion, the use of two aromatic indole groups as hydrophobic shields for coordinated mercury is possible, but it depends on their placements in the linear peptide sequence. On the other hand, computational modeling studies showed that bis(indole) groups in the conformationally constrained **BT3** can effectively act as hydrophobic shields, whereby the dithiolated mercury is 'sandwiched' between two indole rings. The cyclopeptide molecular

Table 1
Calculated energies for the three most stable conformers of the complex Hg-**BT3**.

Structure	$E_{B3LYP-D3}$ (hartree)	E_{ZPV} (hartree) unscaled	$G_{correction}$ (hartree)	ΔG_{solv} (hartree)	G_{soln} (hartree)	ΔG (kJ/mol)
Conformer 1	−3080.10901	0.65514	0.54835	−0.09260	−3079.65326	0.0
Conformer 2	−3080.10881	0.65512	0.54790	−0.09087	−3079.65178	3.9
Conformer 3	−3080.10566	0.65477	0.54708	−0.09281	−3079.65138	4.9

$G_{soln} = (E_{B3LYP-D3} + G_{corr} - E_{ZPV} + 0.96(E_{ZPV})) + \Delta G_{solv}$

template is an attractive structural scaffold, which can be used to position additional auxiliary binding groups to stabilize the mercury complex. The findings of this work will be useful for the rational design of next generation chelators for toxic metal ions such as mercury(II).

4. Experimental

4.1. Materials and methods

HPLC grade acetonitrile and water, sodium hydrogen phosphate and sodium dihydrogen phosphate were purchased from Fisher Scientific (Pittsburgh, Pennsylvania, USA). Mercury(II) chloride (ACS grade) was obtained from Millipore-Sigma (St. Louis, Missouri, USA). Custom designed pentapeptides, **BT1, BT2, and BT3** were purchased from Genscript (Piscataway, New Jersey, USA) at > 98% purity by HPLC. **BT1** (ESI-MS $[M + H]^+$ is 396.1, peptide content = 73.5%), **BT2** ESI-MS $[M + H]^+$ is 525.1, peptide content = 63.3%), and **BT3** (ESI-MS $[M + H]^+$ is 525.1, peptide content = 69.5%). The concentration of these peptide solutions was determined from their UV absorption intensity of tryptophan (ε_{280nm} = 5,690 M^{-1} cm^{-1}). Caution: Mercury compounds are hazardous and should be handled with proper precautions, and they must be disposed in chemical waste containers designated for heavy metals.

4.2. LTQ Orbitrap mass spectrometry

Samples were analyzed on an Orbitrap instrument, the Thermo Fischer Scientific LTQ Orbitrap XL mass spectrometer (Thermo Fisher, San Jose, CA), as described in our previous study.[39] Complexes of the peptides with Hg(II) were evaluated by reacting samples of Hg(II) and peptide solutions at a molar ratio of 1:1 in 5 mM ammonium formate, pH 7 for 30 min. The concentration of Hg(II) and the tetrapeptide were fixed at 10 μM. MS scans were acquired over an *m/z* range of 125–2000. Each sample injection acquired 100 scans. ESI-MS spectra are displayed by setting the base peak at 100% relative abundance, and by labeling the *m/z* value of the most intense peak in each isotopic cluster.

4.3. UV–vis spectroscopy

Reaction mixtures of the peptides titrated with $HgCl_2$ in 50 mM sodium phosphate (pH 7) were studied by UV–vis spectroscopy on a dual beam Shimadzu UV-2401PC series UV–vis spectrophotometer as previously described. UV absorption spectra were acquired at room temperature using a 1 cm path-length quartz cuvette. A 2.5 mL solution consisting of 5 or 10 μM peptide was titrated with aliquots of a 5 mM $HgCl_2$ stock solution at pH 7. The reaction mixture was mixed and stirred for 1 min, followed by an additional 2 min equilibration. The pH of the final reaction mixture was also measured to ensure that the buffer capacity is sufficient to maintain the pH at 7. The UV spectrum arising from the binding of the Hg^{2+} to peptide was obtained by subtracting the background of the peptide in the absence of Hg^{2+}. The change in extinction coefficients at various wavelengths were obtained from the original subtracted data. UV absorption spectra are presented as acquired and are not smoothed. The subtracted spectra are smoothed for clarity purpose, without distorting the original features, by using the Savitzky-Golay method with an average from 12 points.

4.4. Circular dichroism

CD spectroscopic measurements were conducted on a Jasco J-815 Circular Dichroism Spectrometer (Easton, Maryland, USA) equipped with a Peltier temperature controlled cell holder (PTC-423S/C). Spectra were recorded at 25°C using a 1 cm path-length quartz cell with the following parameters: standard sensitivity = 100 mdeg; continuous scanning mode at 50 nm/min; bandwidth = 1.0 nm; response = 4 *sec*; data pitch = 0.1 nm. Peptide solutions were prepared at 5 μM in 5 mM sodium phosphate, pH 7. Each spectrum represents an average of four consecutive scans. The mercury(II) binding reaction mixture was prepared by titrating an aliquot of a 5 mM $HgCl_2$ stock solution in buffer into the respective peptide solution. Molar ellipticity (deg M^{-1} cm^{-1}) was determined using the spectral analysis platform in the Jasco Spectra Manager™ version 2 program (Jasco software, Inc.) as previously described.[21]

4.5. Fluorescence

Fluorescence spectroscopy measurements were carried out on a FluoroMax spectrofluorimeter (Horiba Scientific, New Jersey, USA), equipped with a Peltier temperature controlled cell holder (SGL-POS QNW W/CIR). The fluorescence emission spectra were recorded at 25°C, 35°C, and 45°C by using 10 μM peptide solutions in a 3 mL quartz cell with a path length of 1 cm. The dependency of the fluorescence intensity on quencher concentration was studied by the Stern–Volmer equation: $F_0/F = 1 + K_{SV}[Q]$, where F_0 and F are the fluorescence intensities in the absence and presence of the quencher, respectively. K_{SV} is the Stern–Volmer constant, and [Q] is the concentration of the quencher.[33]

4.6. Computational methods

Low energy conformations for Hg-**BT3** complexes were identified using a Monte Carlo conformational search method followed by minimization. The MMFF molecular mechanics force field was used for gas phase geometry minimizations and energy evaluations. The MMFF force field does not include parameters for Hg^{2+} but uses a default atom type in place of the missing parameters. Regardless, the S—Hg—S moiety structure was constrained to a 180-degree bond angle and 2.45 Å S—Hg bond lengths. The charge on Hg was set as 2+ and the molecular charge set as neutral. Four conformation searches were performed where the peptide ring has two β-turns. Each search differed according to the four possible orientations of the β-turn amide groups by flipping. 50,000 conformations were generated, and the 500 lowest energy structures were saved followed by redundant conformation elimination. Calculations described above were performed with default settings, unless otherwise specified, using Spartan'18.[40] The Spartan optimized conformations were re-optimized using the B3LYP density functional theory method with the SDD basis set and effective-core potential (ECP) on Hg and 6-31G(d) basis set on all other elements. The quasi-relativistic effective-core potential for 60 core electrons was used for mercury atom.[41] The B3LYP functional has been applied previously to obtain quality geometries for $[Hg(II)(SH)_X]^{2-X}$ (X = 1–4) complexes.[34] B3LYP/6-31G(d)/SDD vibrational frequencies were calculated for optimized geometries to ensure characterization as minima having zero imaginary vibrational frequencies.

To estimate the aqueous stability of each complex structure the Gibbs energy in solution (G_{soln}) for each was calculated by summing the gas phase Gibbs energy (G_{gas}) and Gibbs energy of solvation (ΔG_{solv}).

$$G_{soln} = G_{gas} + \Delta G_{solv}$$

To obtain the gas phase Gibbs energy (G_{gas}), structures were energy evaluated in vacuum at the B3LYP-D3/6–311++G(d,p)/aug-cc-pVTZ-PP level with a 6–311++G(d,p) basis set on non-metal atoms and aug-cc-pVTZ-PP basis set and ECP on mercury.[42] These energy evaluations include the dispersion energy correction from Grimme's D3 method.[43] The B3LYP/6-31G(d)/SDD zero-point vibrational energies were scaled by 0.960.[44] The Gibbs energy of solvation (ΔG_{solv}) in water was determined using the SMD model[35] by performing a self-consistent PCM calculation using the B3LYP/6-31G(d)/SDD method using default solvent cavity values. The Gaussian16 software program was used for all geometry optimizations, frequency analysis and Gibbs energy of solvation values.[45]

Declaration of Competing Interest

The authors declare that they have no known competing financial interests or personal relationships that could have appeared to influence the work reported in this paper.

Acknowledgements

This work was supported by the National Science Foundation grant CHE-1831020.

Appendix A. Supplementary material

Supplementary data to this article can be found online at https://doi.org/10.1016/j.bmc.2021.116296.

References

1 World Health Organization; Ten Chemicals of Major Health Concerns: Geneva, Switzerland, 1-4. https://www.who.int/ipcs/assessment/public_health/chemicals_phc/en/.
2 Bernhoft RA. Mercury Toxicity and Treatment: A Review of the Literature. *J Environ Public Health*. 2012;2012, 460508.
3 Cariccio VL, Sama A, Bramanti P, Mazzon E. Mercury Involvement in Neuronal Damage and in Neurodegenerative Diseases. *Biol Trace Elem Res*. 2019;187(2):341–356.
4 Ajsuvakova OP, Tinkov AA, Aschner M, et al. Sulfhydryl groups as targets of mercury toxicity. *Coord Chem Rev*. 2020;417.
5 George GN, Prince RC, Gailer J, et al. Mercury Binding to the Chelation Therapy Agents DMSA and DMPS and the Rational Design of Custom Chelators for Mercury. *Chem Res Toxicol*. 2004;17(8):999–1006.
6 Rabenstein DL, Backs SJ, Isab AA. Nuclear magnetic resonance studies of the complexation of trimethyllead by glutathione in aqueous solution and in intact human erythrocytes. *J Am Chem Soc*. 1981;103(10):2836–2841.
7 Nogara PA, Oliveira CS, Schmitz GL, et al. Methylmercury's chemistry: From the environment to the mammalian brain. *Biochim Biophys Acta, Gen Subj*. 2019;1863(12), 129284.
8 Yamashita MM, Wesson L, Eisenman G, Eisenberg D. Where metal ions bind in proteins. *Proc Natl Acad Sci U S A*. 1990;87(15):5648–5652.
9 Bal W, Chmurny GN, Hilton BD, Sadler PJ, Tucker A. Axial Hydrophobic Fence in Highly-Stable Ni(II) Complex of Des-Angiotensinogen N-Terminal Peptide. *J Am Chem Soc*. 1996;118(19):4727–4728.
10 Gallivan JP, Dougherty DA. Cation-pi interactions in structural biology. *Proc Natl Acad Sci U S A*. 1999;96(17):9459–9464.
11 Dougherty DA. Cation-pi interactions in chemistry and biology: a new view of benzene, Phe, Tyr, and Trp. *Science*. 1996;271(5246):163–168.
12 Dougherty DA. The Cation−π Interaction. *Accounts Chem Res*. 2013;46(4):885–893.
13 Ma JC, Dougherty DA. The Cation-pi Interaction. *Chem Rev*. 1997;97(5):1303–1324.
14 Gokel GW. Indole, the aromatic element of tryptophan, as a pi-donor and amphiphilic headgroup. *Int Congr Ser*. 2007;1304:1–14.
15 Franz KJ. Copper shares a piece of the pi. *Nat Chem Biol*. 2008;4(2):85–86.
16 Craven TW, Cho MK, Traaseth NJ, Bonneau R, Kirshenbaum K. A Miniature Protein Stabilized by a Cation-pi Interaction Network. *J Am Chem Soc*. 2016;138(5):1543–1550.
17 Kamiyama T, Miura T, Takeuchi H. His-Trp cation-pi interaction and its structural role in an alpha-helical dimer of HIV-1 Vpr protein. *Biophys Chem*. 2013;173–174:8–14.
18 Okada A, Miura T, Takeuchi H. Protonation of Histidine and Histidine−Tryptophan Interaction in the Activation of the M2 Ion Channel from Influenza A Virus. *Biochemistry*. 2001;40(20):6053–6060.
19 Isaac M, Denisov SA, Roux A, et al. Lanthanide Luminescence Modulation by Cation-pi Interaction in a Bioinspired Scaffold: Selective Detection of Copper(I). *Angew Chem Int Ed Engl*. 2015;54(39):11453–11456.
20 Chadha N, Silakari O. Indoles as therapeutics of interest in medicinal chemistry: Bird's eye view. *Eur J Med Chem*. 2017;134:159–184.
21 Ngu-Schwemlein M, Merle J, Meeker W, Risdon-Langdon K, Nixon T. Evaluating the involvement of tryptophan on thiolated peptide-mercury(II) complexes: Cation-pi interactions. *Inorg Chim Acta*. 2020;506, 119552.
22 Pearson RG. Hard and Soft Acids and Bases. *J Am Chem Soc*. 1963;85(22):3533–3539.
23 Xu Y, Zhang X, Yergey AL. Electrospray ionization of copper—Glycine solutions. *J Am Soc Mass Spectr*. 1996;7(1):25–29.
24 Pan J, Xu K, Yang X, Choy W-Y, Konermann L. Solution-Phase Chelators for Suppressing Nonspecific Protein−Metal Interactions in Electrospray Mass Spectrometry. *Anal Chem*. 2009;81(12):5008–5015.
25 Wright JG, Natan MJ, MacDonnel FM, Ralston DM, O'Halloran TV. Mercury(II)—Thiolate Chemistry and the Mechanism of the Heavy Metal Biosensor MerR. *Prog Inorg Chem*. 2007:323–412.
26 Seneque O, Rousselot-Pailley P, Pujol A, et al. Mercury Trithiolate Binding (HgS3) to a de Novo Designed Cyclic Decapeptide with Three Preoriented Cysteine Side Chains. *Inorg Chem*. 2018;57(5):2705–2713.
27 Yorita H, Otomo K, Hiramatsu H, Toyama A, Miura T, Takeuchi H. Evidence for the cation-pi interaction between Cu^{2+} and tryptophan. *J Am Chem Soc*. 2008;130(46):15266–15267.
28 Pires S, Habjanič J, Sezer M, Soares CM, Hemmingsen L, Iranzo O. Design of a Peptidic Turn with High Affinity for HgII. *Inorg Chem*. 2012;51(21):11339–11348.
29 Sreerama N, Woody RW. Circular Dichroism of Peptides and Proteins. In: Berova N, Nakanishi K, Woody RW, eds. *Circular Dichroism: Principles and Applications*. Wiley-VCH; 2000:601–620.
30 Perczel A, Hollosi M, Turns. In: Fasman GD, editor. Circular Dichroism and the Conformational Analysis of Biomolecules, Plenum; 1996. p. 285-380.
31 Masuhara H, Shioyama H, Saito T, Hamada K, Yasoshima S, Mataga N. Fluorescence quenching mechanism of aromatic hydrocarbons by closed-shell heavy metal ions in aqueous and organic solutions. *J Phys Chem*. 1984;88(24):5868–5873.
32 Xue Y, Davis AV, Balakrishnan G, et al. Cu(I) recognition via cation-π and methionine interactions in CusF. *Nat Chem Biol*. 2008;4(2):107–109.
33 Lakowicz JR. *Principles of Fluorescence Spectroscopy*. 3rd ed. New York: Springer Science and Business Media, LLC; 2006:278–318.
34 Watts J, Howell E, Merle JK. Theoretical studies of complexes between Hg(II) ions and l-cysteinate amino acids. *Int J Quantum Chem*. 2014;114(5):333–339.
35 Hutchinson EG, Thornton JM. A revised set of potentials for beta-turn formation in proteins. *Protein Sci*. 1994;3(12):2207–2216.
36 Nishio M, Umezawa Y, Fantini J, Weiss MS, Chakrabarti P. CH-pi hydrogen bonds in biological macromolecules. *PCCP*. 2014;16(25):12648–12683.
37 Brandl M, Weiss MS, Jabs A, Suhnel J, Hilgenfeld R. C-H...pi-interactions in proteins. *J Mol Biol*. 2001;307(1):357–377.
38 Nishio M. The CH/pi hydrogen bond in chemistry. Conformation, supramolecules, optical resolution and interactions involving carbohydrates. *PCCP*. 2011;13(31):13873–13900.
39 Merle J, Mazlo J, Watts J, Moreno R, Ngu-Schwemlein M. Reaction mixture analysis by ESI-MS: Mercury(II) and dicysteinyl tripeptide complex formation. *Int. J. Mass Spectr*. 2018;426:38–47.
40 Spartan'18, Wavefunction, Inc.: Irvine, CA; 2020.
41 Andrae D, Häußermann U, Dolg M, Stoll H, Preuß H. Energy-adjustedab initio pseudopotentials for the second and third row transition elements. *Theor Chim Acta*. 1990;77(2):123–141.
42 Peterson KA, Puzzarini C. Systematically convergent basis sets for transition metals. II. Pseudopotential-based correlation consistent basis sets for the group 11 (Cu, Ag, Au) and 12 (Zn, Cd, Hg) elements. *Theor. Chem. Acc*. 2005;114(4):283–296.
43 Grimme S, Antony J, Ehrlich S, Krieg H. A consistent and accurate ab initio parametrization of density functional dispersion correction (DFT-D) for the 94 elements H-Pu. *J Chem Phys*. 2010;132(15), 154104.
44 Johnson III, RD. NIST Computational Chemistry Comparison and Benchmark Database NIST Standard Reference Database Number 101 Release 20. http://cccbdb.nist.gov (accessed April 1, 2021).
45 Gaussian 16, Revision B.01, Wallingford CT; 2016.